Ordering Dynamics of a Symmetric Polystyrene-*block*-polyisoprene. 2. Real-Space Analysis on the Formation of Lamellar Microdomain

Naoki Sakamoto and Takeji Hashimoto*

Department of Polymer Chemistry, Graduate School of Engineering, Kyoto University, Kyoto 606-8501, Japan

Received January 12, 1998; Revised Manuscript Received April 7, 1998

ABSTRACT: We have investigated the morphology developed in the ordering process for a nearly symmetric polystyrene-*block*-polyisoprene diblock copolymer when the copolymer is rapidly brought from a disordered state to an ordered state. The ordering process was explored as a function of time and temperature primarily by transmission electron microscopy (TEM): the microdomain structures formed during the ordering process were observed on specimens frozen at particular times in the ordering process. Complementary small-angle X-ray scattering experiments on the specimens before and after freezing assured that the structures existed before freezing were really conserved in the frozen specimens. The TEM observations showed that the ordered grains of the lamellar microdomain were developed in the matrix of the disordered phase and that the grains grew at the expense of the disordered phase at all the temperatures covered in this study. The coexistence of the ordered and disordered phases suggests that this ordering is a nucleation and growth process. We found that the shape of the lamellar grains developed in the disordered phase were very anisotropic at all stages and temperatures covered in this study: the size along the lamellar normals was much larger than that parallel to the lamellar interfaces. Furthermore in the early stage of the ordering, the lamellae formed in the ordered grains were perforated but they eventually become solid lamellae.

I. Introduction

Order−disorder transition (ODT) of block copolymer melts has been extensively studied both theoretically and experimentally.[1,2] About 2 decades ago, Leibler[3] developed the Landau type mean-field theory based on the random phase approximation (RPA). The theory predicts that the ODT for a symmetric block copolymer with respect to composition belongs to a second-order phase transition, while the ODT for asymmetric blocks belongs to a first-order phase transition.

The theory predicts that if the Flory−Huggins segmental interaction parameter, χ, changes with the absolute temperature, T, according to $\chi = A + B/T$, where A and B are constant, a reciprocal of a maximum elastic scattered intensity, I_m^{-1}, and a square of half-width at half maximum of the peak, σ_q^2, should change linearly with $1/T$ in the disordered state. However, as pointed out by Leibler, the behavior of the system near the ODT deviates from this mean-field prediction, because the thermal fluctuations that were neglected in the mean-field theory play an important role at temperatures close to the ODT. Fredrickson and Helfand (FRH)[4] took into account this thermal fluctuation effect (Brazovskii effect[5]) on the ODT and predicted that the ODT becomes a first-order phase transition even for a symmetric block copolymer.

Since the FRH theory has been proposed, many investigators reported the experimental evidence that the behavior of block copolymers deviates from Leibler's mean-field theory near the ODT by using static small angle X-ray (SAXS)[6−9] and neutron scattering (SANS).[10,11] These static experimental results proved importance of the thermal fluctuations (random thermal force) on the ODT and supported the FRH theory on the fluctuation-induced first-order phase transition. The thermal fluctuations give a strong effect on the ordering mechanism: the ordering occurs via the nucleation-growth (NG) process rather than spinodal decomposition (SD) process, as elaborated by Fredrickson and Binder (FRB).[12]

Following the theory of FRB, the dynamics of the ODT for block copolymers, especially the ordering process for systems quenched from the disordered state to the ordered state, have been experimentally studied by means of time-resolved SAXS,[13−17] low-frequency rheology,[18,19] and depolarized light scattering.[20,21] However the ordering process has not been observed so far in real space by transmission electron microscopy (TEM) etc., except for our previous short communication or note.[15−17] Hence almost no real-space information is available at present for the formation and development of the microdomain structure from the disordered state.

In the short communication and note, we presented briefly the TEM results, showing the existence of anisotropic grains of lamellae[15] or existence of an isolated anisotropic grain of lamellae[16] in the ordering process very close to the ODT. These experimental results were qualitatively interpreted in the context of the NG theory developed by FRB[12] and Hohenberg and Swift (HS).[22] However these results were obtained only at a particular time in the ordering process at a particular temperature close to the ODT. The documentation for the experimental evidence was also not necessarily completed, because it is a brief report.

In this series of papers, we aim to describe a full account of the ordering process and the ordering structures, not only the ordering at a particular time and at a particular temperature as described in the previous papers[15,16] but also the ordering processes and the ordered structures as a function of time and temperature. The ordering was induced by the T-drop method, according to which the SI diblock copolymer OSI-3 (see Table 1) was quenched from the initial temperature T_i ($\geq T_{MF}$) to the final temperatures T_f's ($< T_{ODT}$) where the isothermal ordering is explored. Here T_{MF} is the

S0024-9297(98)00037-0 CCC: $15.00
Published on Web 05/23/1998

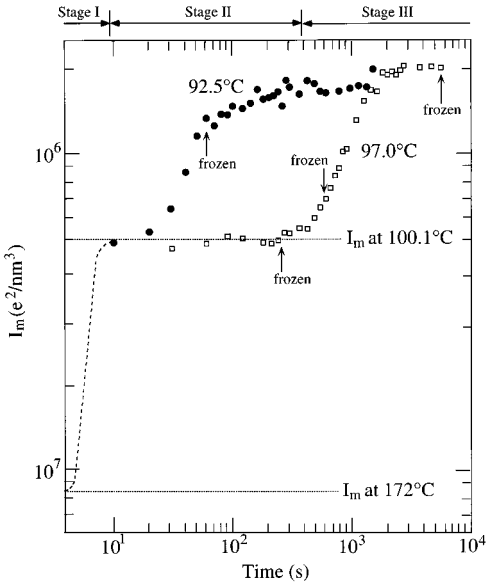

Figure 1. Time evolution of I_m after T-drop from 172 °C above the T_{MF} ($\ll T_{ODT}$) to 97.0 and 92.5 °C below the T_{ODT}. The dash line shows the expected time evolution of I_m at $t < 10$ s, though it could not be observed. The arrows show the time when the TEM observations in Figures 3b, 5, 6, and 7 were made. The two horizontal dotted lines show the equilibrium values at 172 and 100.1 °C, the latter of which is the upper bound of ODT, that is, $T_{ODT,\,H}$. The three stages of the ordering process for 97.0 °C are shown on the top of this figure.

crossover temperature from the mean-field disordered state to non-mean-field disordered state: above T_{MF}, the scattering behaviors are described, to a good approximation, by the mean-field theory.[9]

In part 1 of this series,[23] we discussed the ordering processes via the NG process at various times (t) and temperatures (T) as observed by a systematic time-resolved SAXS experiment. In that paper, we defined the quench depth, ΔT, as

$$\Delta T \equiv T_{ODT,H} - T_f \qquad (1)$$

where $T_{ODT,H}$ is the onset temperature of the ordering from the disordered state or the temperature above which the ordered phase completely disappears, obtained from the static SAXS experiment.[23] As shown in Table 1, the $T_{ODT,H}$ of OSI-3 is 100.1 °C. In part 1, we found that the ordering at shallow quenches (at 92.5 $\le T_f \le$ 97.0 °C, i.e., at 7.6 $\ge \Delta T \ge$ 3.1 °C) proceeds with the essentially same mechanism as follows (see Figure 1 as will be described immediately below): (I) After T-drop, the profile changes from the equilibrium at T_i = 172 °C to that at 100.1 °C, which is very close to the T_{ODT} in the disordered state, within the shortest time covered in this experiment. The change in this stage corresponds to the relaxation of the thermal concentration fluctuations from T_i = 172 °C to $T_{ODT,H}$ = 100.1 °C. (II) The SAXS profiles stay there for a certain incubation period (for 400 s at 97.0 °C). (III) After the incubation period, the SAXS profile starts to change with t. In stage III, there are two characteristic wavenumbers q_{cS} and q_{cL}: the scattered intensity increases at $q_{cS} < q < q_{cL}$ and decreases at $q > q_{cL}$ or $q < q_{cs}$. The change in this stage corresponds to the formation of the lamellar grains at the expense of the disordered phase.

Figure 1 represents the time evolution of the peak scattered intensity, I_m, after T-drop from T_i = 172 °C ($\ge T_{MF} \gg T_{ODT}$) to T_f = 97.0 and 92.5 °C ($< T_{ODT}$). These data typically represent the trend of the time-evolution curve obtained between 92.5 and 97.0 °C. The arrows shows the time when we made the TEM observations as will be discussed later in this paper. These data are presented here in order to indicate clearly the states when the morphology was explored. The data themselves will not be analyzed here. The detailed analysis should be referred to part 1 of this series.[23] The two horizontal dotted lines show the equilibrium values at 172 and 100.1 °C; the latter temperature is the temperature just above the T_{ODT}. The time evolution of I_m at 97.0 °C clearly shows the three stages of the ordering described above. The time evolution of I_m at 92.5 °C also shows a similar trend to that at 97.0 °C. Though the incubation period was not obviously observed, we consider that it exists at a time scale shorter than 20 s for the following reason: The early stage of the ordering process at various temperatures (at 92.5 $\le T_f \le$ 97.0 °C) can be scaled with the temperature-dependent half-time ($t_{1/2}$):[23] the time-evolution curves in the early stage at 97.0 and 92.5 °C in Figure 1 can be superposed if the curve at 92.5 °C is shifted to the right-hand side.

In part 1 we determined also the volume fraction $X_{order}(t;T)$ of the ordered phase as a function of t and T from the time-resolved SAXS profiles. The results were used for Avrami analysis; the Avrami analysis showed the Avrami exponent (n) of $3 < n < 4$, suggesting a possibility of three-dimensional anisotropic homogeneous nucleation. In this paper the TEM results were occasionally used only to show the anisotropic features of the ordered grains in the disordered matrix for the interpretation of Avrami exponent. However no further details about morphologies developed in the ordering processes were discussed.

In this paper (part 2 of this series), we aim to elucidate morphological details of the ordering process. The morphology during the ordering process was investigated by TEM on the specimens frozen at various times during the ordering at various temperatures.

Table 1. Molecular Characteristics of the Polystyrene-*block*-polyisoprene Diblock Copolymers

code	M_n	M_w/M_n	f_{PS}	T_{ODT} (°C)[a]	T_{MF} (°C)
OSI-3	1.5×10^4	1.02	0.45	$98.5 \le T_{ODT} \le 100.1$	170

[a] The T_{ODT} was determined by the static SAXS experiment.[9] In the cooling cycle, the ordering starts at 100.1 °C and completes at 98.5 °C: the ordered and disordered phases coexist between 98.5 and 100.1 °C within the time scale of this experiment (for ca. 6 h). In this time scale of experiments we observed almost no hysterisis: during the heating, the disordering starts at 98.5 °C and completes at 100.1 °C. The precise description of the ODT in OSI-3 was presented in ref 23.

II. Experimental Methods

The SI diblock copolymer, coded as OSI-3, used in this work is the same as that in part 1.[23] Its molecular characteristics are listed in Table 1, where M_n, M_w, and f_{PS} are the number- and weight-average molecular weight, and the volume fraction of polystyrene (PS) block in the SI diblock copolymer, respectively.

In order to explore the ordering process of a nearly symmetric diblock copolymer, the T-drop measurements were conducted by quenching the melt from T_i = 172 °C, which is far above T_{ODT} and slightly higher than T_{MF} to various temperatures T_f in the ordered state. In this series of the study, the quenching process was done as follows: first the specimen placed in a small aluminum cell was put in the heater block, the temperature of which was controlled at the

initial temperature, T_i, then the cell was rapidly transferred manually into another heater block that was set to the optical path of the incident X-ray beam and regulated at T_f. The time-resolved SAXS measurements were started and time zero was set when the cell was placed into the heater block at T_f. The details of the SAXS measurements may be found in part 1 of this series.[23] Here we only use the SAXS data primarily for the purpose of clarifying the state at which the morphological study with TEM was conducted.

The structures developed during the ordering process were observed by TEM. After a T-drop from T_i to T_f with the same method described above, the specimens at various times t and temperatures T_f were put into an ice−water bath at 0 °C. Because the glass transition temperature (T_g) of the block copolymer in the disordered state or PS microdomains in an ordered state is higher than 0 °C, we can freeze the structure at the moment when the system was put into ice−water. Thus we can observe the structures frozen during the ordering by TEM. The frozen specimens at 0 °C were subjected to microtoming into the ultrathin sections of ca. 50 nm thickness at −85 °C with a Reichert-Jung ultracut E together with a cryogenic unit FC 4E and a glass knife. The ultrathin sections were quickly picked up on 400-mesh copper grids and immediately subjected to staining with osmium tetraoxide vapor at room temperature for about a half day. TEM observation was made with a Hitachi H-600 transmission microscope at 100 kV.

In this paper, we will show the results obtained by the T-drop from T_i = 172 °C to T_f = 97.0 and 92.5 °C. These temperatures are considered to be representative, because they correspond to the upper and lower bands of the temperature interval, over which the Avrami analysis was conducted[23] and the time evolution of the peak SAXS intensity in the early stage of the ordering process at various temperatures was scaled with respect to the temperature-dependent half-time $t_{1/2}$.[23] The TEM observations were done at 330, 630, and 7285 s after T-drop to 97.0 °C and at 60 s after T-drop to 92.5 °C (see the arrows in Figure 1). Moreover, we made a TEM observation on the structure at 100.1 °C which is just above T_{ODT} in the disordered state by freezing the specimen with the same method as that described above.

III. Experimental Results

III-1. TEM Observations at 100.1 °C. It is quite interesting that the value I_m in the incubation period is close to the I_m at 100.1 °C equal to $T_{ODT,H}$ (see Figure 1). This suggests that the structures at 100.1 °C should be essentially identical to those in the incubation period at 97.0 °C. In fact, the SAXS profile equilibrium at 100.1 °C was found to be identical to that measured in the incubation period at least near the scattering maximum (see Figure 6 of ref 23). Our previous static SAXS analysis on this sample showed that the mean-field spinodal temperature, $T_{s,MF}$, determined is equal to ca. 140 °C. This means that the disordered phase at 100.1 °C becomes thermodynamically unstable, and hence the system should order via spinodal decomposition (SD), if the thermal fluctuations (random thermal forces) are negligible. As a matter of fact, the system stays disordered due to the thermal fluctuations. Thus we can define the structures at 100.1 °C as the **fluctuation-induced disordered structure** (**D_F**). It is quite natural to raise the following questions: What kind of characteristics does the D_F structure have in real space? Is the D_F structure really equivalent to the structure in the incubation period at 97.0 °C?

In order to address the above questions, TEM observations were performed for the specimens frozen with ice−water from the equilibrium state at 100.1 °C or at a particular time during the ordering. To check whether

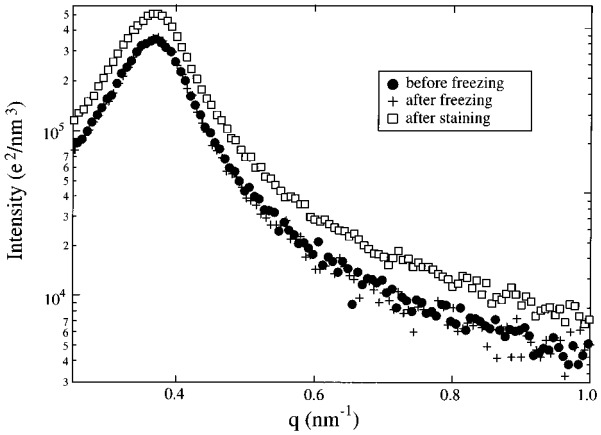

Figure 2. Comparison of the SAXS profiles measures before (●) and after freezing (+) from 100.1 °C and after staining (□) by osmium tetraoxide vapor.

or not the freezing and staining processes changed the structure, the SAXS profiles measured before and after freezing, and that after staining with osmium tetraoxide are compared. Typical results are demonstrated in Figure 2, which shows the effect of freezing from the D_F state at 100.1 °C on the profiles. The profiles before (filled circles) and after freezing (crosses) are completely identical. Moreover the shape of the profile after staining (squares) is equal to the two profiles described above, though the intensity level is different. It means that the freezing and staining processes did not change the structure. The difference of the intensity level between the profile after staining and the other two profiles before staining results from the change of the electron density difference between PS-rich and polyisoprene (PI)-rich domains that result from the frozen thermal concentration fluctuations. Osmium tetraoxide selectively reacts with PI chains, consequently making electron density difference between the PI- and PS-rich domains larger. Using the method as described above, we confirmed that the freezing-in process does not cause an additional ordering or any changes in the structure occurring before freezing, whenever we applied this method.

Figure 3a gives the TEM picture for the specimen frozen from the state at 100.1 °C, which is equal to the $T_{ODT,H}$. Figure 3b, which is aimed to demonstrate a direct comparison with Figure 3a, will be discussed later in section III-2. The inset shows a magnified image. It is noted in Figure 3a that a three-dimensional (3D) bicontinuous structure composed of domains rich in PS (bright) and PI chains (dark) exists in the frozen disordered state. The bright and dark domains that manifest the frozen thermal concentration fluctuations have only a short-range order, and their spatial arrangement is directionally independent. In order to give evidence, in addition to that in Figure 2, that the structure shown in Figure 3a is not an artifact but really illuminates the frozen structure in the disordered state at 100.1 °C, we present in Figure 4 the two-dimensional fast Fourier transformation (FFT) pattern of Figure 3a. The FFT pattern shows an almost isotropic ring, consistent with the fact that the scattering from block copolymers in the disordered state gives an isotropic pattern with a single maximum. Furthermore the position of the maximum in Figure 4, i.e., the characteristic wavenumber for the dominant mode of the Fourier component of the fluctuations, is almost same

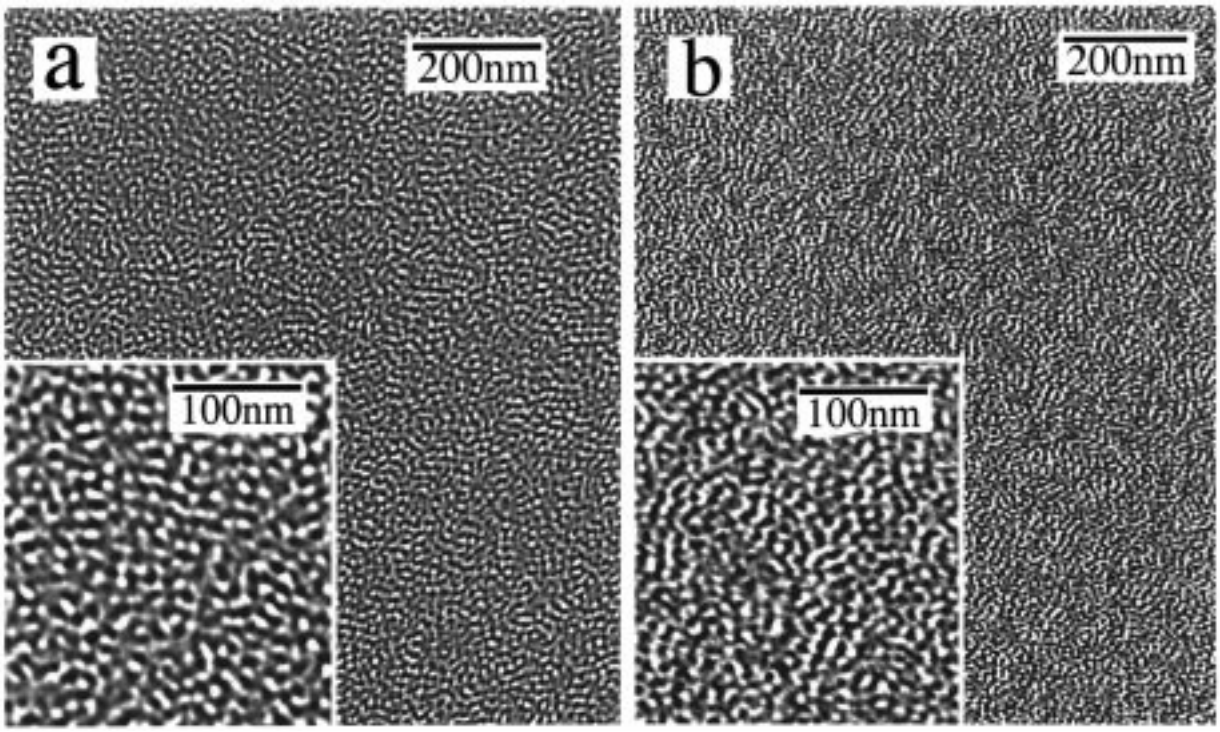

Figure 3. Transmission electron micrograph for the specimen frozen from the disordered state at 100.1 °C, which is equal to $T_{ODT,H}$ (a), and that for the specimen frozen at 330 s after T-drop to 97.0 °C (b). The inset shows a magnified micrograph.

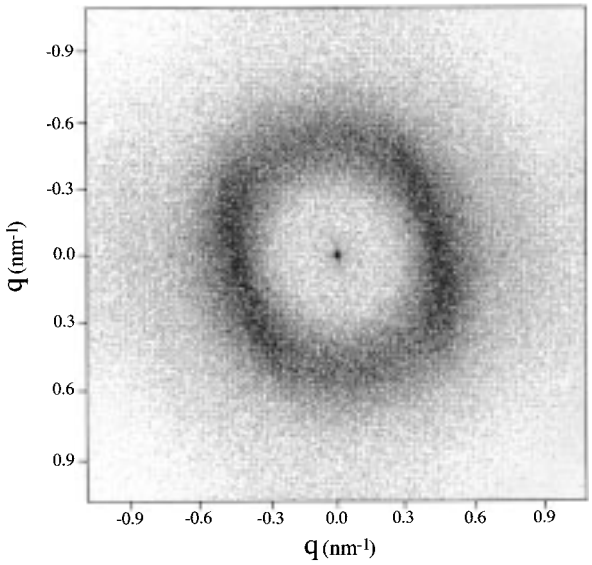

Figure 4. FFT pattern obtained from the image shown in Figure 3a.

as the scattering vector, q_m, at the maximum in the SAXS profile at 100.1 °C in Figure 2, suggesting that the periodicity of the bicontinuous structure in Figure 3a is same as that of the concentration fluctuations in the disordered state at 100.1 °C. Thus we can conclude that the structure in Figure 3a truly reflects the frozen thermal concentration fluctuations in the disordered state at 100.1 °C and an instantaneous picture for the D_F structure. The D_F structure at 100.1 °C is a dynamical object such that the two domains appear, disappear, and are exchanged for each other with a certain relaxation time, keeping their characteristic spacing constant.

III-2. TEM Observations after T-Drop at 97.0 °C. The TEM picture for the specimen frozen at 330 s after quenching to 97.0 °C was shown in Figure 3a of ref 16. Note that the I_m at 330 s still remains equal to the equilibrium value at 100.1 °C, and hence the system is in a incubation period (see Figure 1). In order to facilitate the comparison of the structure existing in the incubation period with the D_F structure at $T_{ODT,H}$, we show the this structure in Figure 3b. We can really find that the two structures shown in Figure 3 are identical, revealing that the system has the D_F structure even in the incubation period of time.

The TEM micrograph at 630 s after T-drop to 97.0 °C is given in Figure 5. Although the corresponding TEM was shown and discussed elsewhere,[16] we wish to show it here in order to make a comparison with the morphology obtained during the ordering at T_f = 92.5 °C (see Figure 7 later) easy, as the comparison is expected to give very fundamental and important pieces of information. It is interesting to note in Figure 5 that a lamellar grain with a well-defined interface exists in the matrix of the less ordered phase, and the less ordered phase has structures very similar to those in Figure 3, indicating that the ordered phase having a lamellar structure and the disordered phase having the D_F structure coexist at 630 s. In fact, we can proposed that the disordered phase has a structure equivalent to the D_F structure by combining the results obtained here in this work with the SAXS results reported in the companion paper.[23] This is because in the companion paper it was found that the net SAXS profile at 630 s after T-drop to 97.0 °C is decomposed into the profile from the disordered phase at 100.1 °C and that obtained for fully ordered structure at 97.0 °C. Furthermore, we should emphasize that the lamellar grain existing in the disordered phase has an anisotropic shape: it is highly elongated toward the direction parallel to lamellar normal **n**, as illustrated in the sketch on the left bottom corner of the micrograph. The existence of a small number of lamellar grains causes a slight increase of

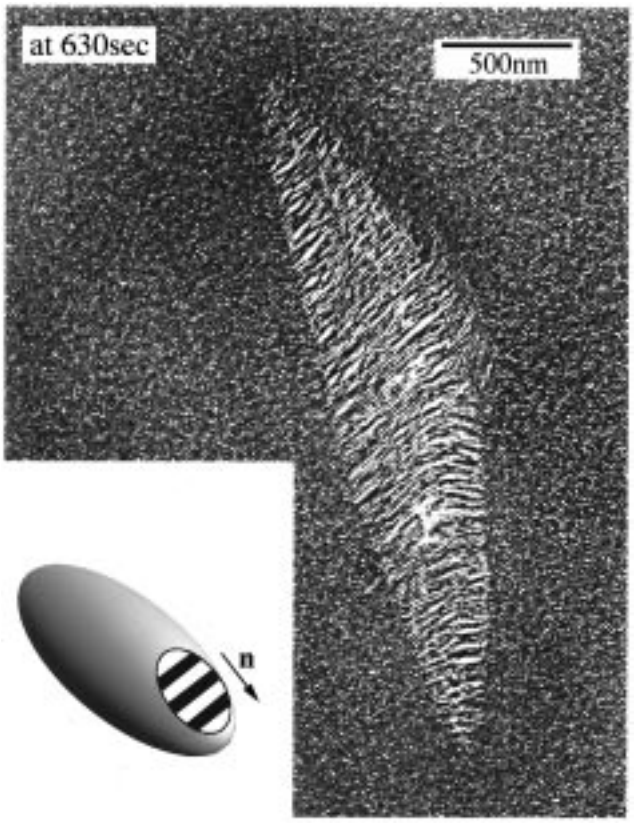

Figure 5. Transmission electron micrograph for the specimen frozen at 630 s after T-drop to 97.0 °C. The inset shows the schematic representation of the ordered lamellar grain developed in the matrix of the disordered phase.

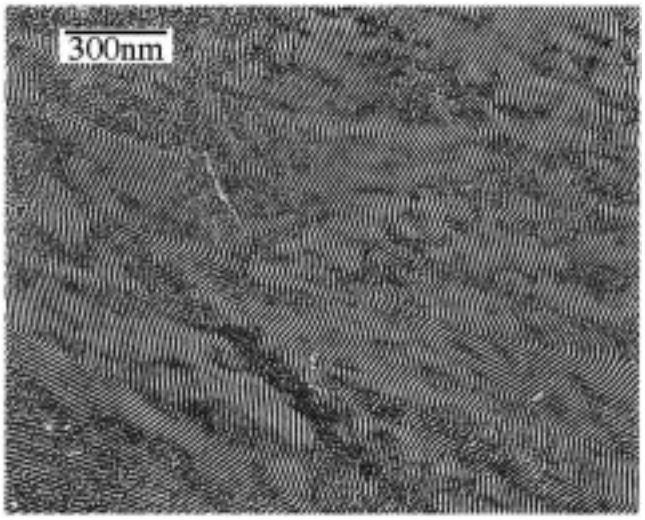

Figure 6. Transmission electron micrograph for the specimen frozen at 7285 s after T-drop to 97.0 °C.

I_m from the I_m value in the incubation period (Figure 1). As time elapses, a number of lamellar grains increase and they form a network type structure in the disordered phase.

Figure 6 gives the TEM picture at 7285 s after quenching to 97.0 °C. Note that the I_m at 7285 s reaches a constant value in Figure 1. In Figure 6, the lamellar structure fills the entire sample space, indicating that the ordering is almost completed. The close observation of Figure 6 reveals that the sample space is filled with grains having such anisotropic grains as shown in Figure 5. Thus a memory built up in the ordering process appears to remain in the solidified specimen.

III-3. TEM Observation at 92.5 °C. The TEM micrograph at 60 s after quenching to 92.5 °C is shown in Figure 7a. The right panel shows a high-magnified image of the lamellar grains. To highlight the lamellar grains, the black and white images were translated into the color images in Figure 7b. The gradations from black and white and that from violet to red are composed of 256 intensity levels. The brightness and color distributions should qualitatively correspond to the concentration fluctuations of PS and PI block chains: It is impressive to note that there appears to be a quite broad distribution in the amplitude of the concentration fluctuations, though this information is still very qualitative.

The coexistence of the ordered and disordered phases is also seen in Figure 7, obtained at a deeper quench than that employed in Figure 5. It is interesting to note that the size of the grain is much smaller than that at 97.0 °C, but nevertheless the grains have anisotropic shape with a large aspect ratio in this case as well: the dimension normal to the lamellar interfaces is much larger than that parallel to the interfaces, as seen in Figure 5. It is also noted that more of the ordered grains are seen in Figure 7 compared with the case of Figure 5, reflecting that the scattered intensity level for the specimen frozen at 60 s after T-drop to 92.5 °C is higher than that for the specimen frozen at 630 s after T-drop to 97.0 °C (see Figure 1).

IV. Discussion

IV-1. Structure Formed in the Disordered State Very Close to the ODT: Fluctuation-Induced Disordered Structure (D_F). In this section, we will analyze the structure in the disordered state at $T_{ODT,H}$, that is, the D_F structure shown in Figure 3a. Although the main purpose in this paper is the real-space analysis, in order to obtain a deeper understanding of the D_F structure captured by the real-space analysis, we will present below the discussion with the scattering profiles as well.

It may seem surprising at first glance that the D_F structure shown in Figure 3a resembles a 3D-bicontinuous structure observed for phase-separated polymer mixtures with equal phase volumes, because any domain structures are not expected to exist in the disordered state. However we interpret the bicontinuous structure as the one reflecting the frozen thermal concentration fluctuations with a significant size in the amplitude. The large amplitude of the fluctuations gives rise to a significant composition difference, which in turn gives rise to a significant contrast after the selective staining with O_SO_4 as shown in Figure 3a.

We speculate that the concentration fluctuations at 100.1 °C could be frozen, because their lifetime may be sufficiently long compared with the time required for freezing them by quenching the specimen in ice−water. It is worthy of note that we failed to freeze the structure in the disordered state at 172 °C, which is higher than T_{MF}: the SAXS profile measured after quenching the specimen into ice−water was much sharper than that at 172 °C in the equilibrium state. It suggests that the relaxation time of the concentration fluctuations in the mean-field disordered state at 172 °C is shorter than the time required for the freezing process. Consequently the structure obtained after freezing from 172 °C was nothing other than the D_F structure itself.

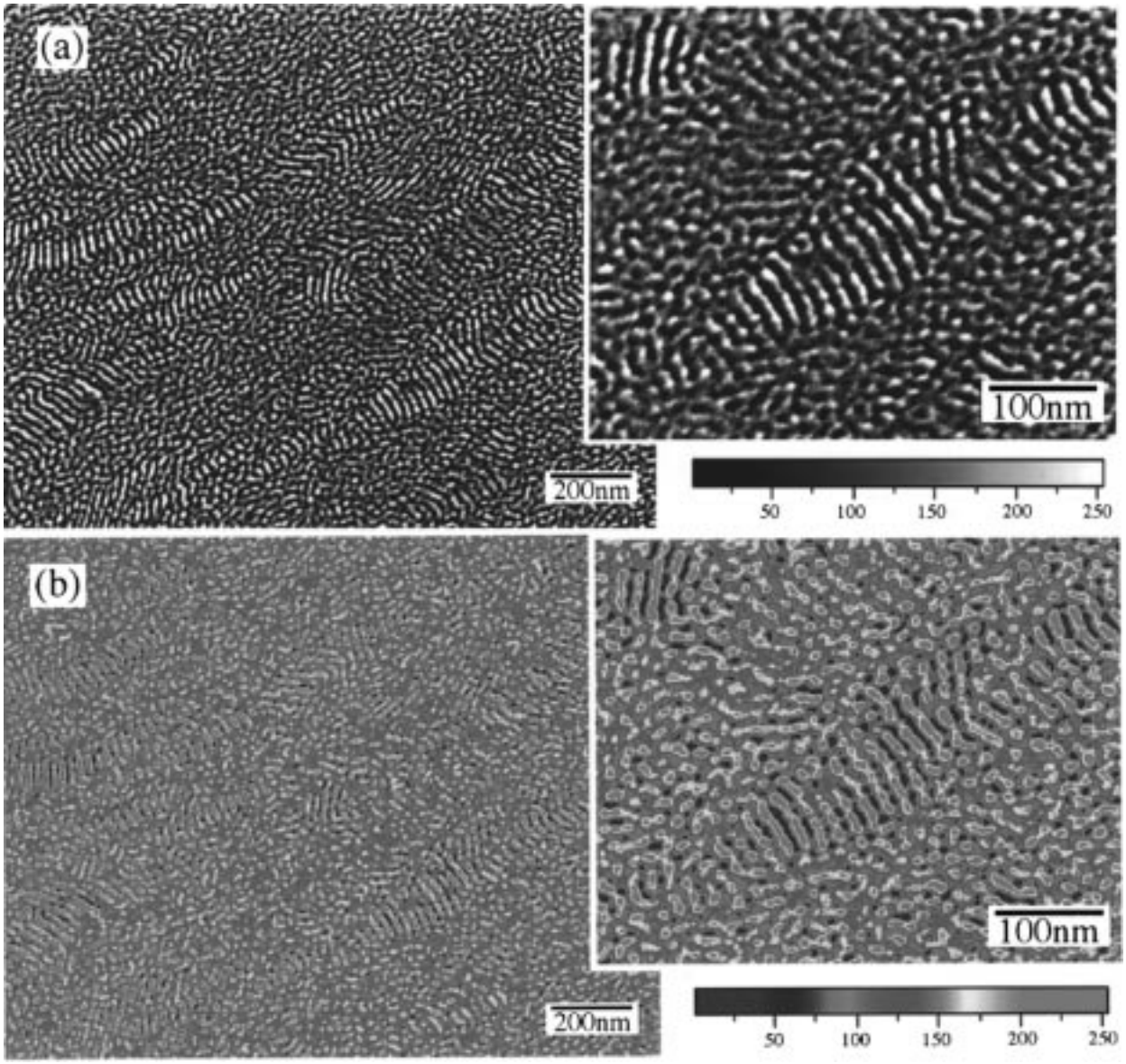

Figure 7. (a) Transmission electron micrograph for the specimen frozen at 60 s after T-drop to 92.5 °C. The right panel shows the magnified micrograph. To highlight the lamellar grains, the black and white images in panel a are translated into the color images in panel b. The gradations from black and white and that from violet to red are composed of 256 intensity levels. The gray and color scales on the bottom right in parts a and b show the brightness and color corresponding to the each intensity level, respectively.

The D_F structure shown in Figure 3a is very similar to the spongelike structure, that is, the 3D-bicontinuous phase-separating structure observed in the late stage spinodal decomposition (SD) for polymer mixtures with equal phase volumes.[24,25] In order to gain a better understanding of the D_F structure, we will try to compare below the D_F structure with the spongelike structure. Bates et al.[10] made a scaling analysis for the SANS profile obtained from the symmetric poly(ethyleneepropylene) (PEP)-*block*-poly(ethylethylene) (PEE) diblock copolymer (coded as PEP-PEE-5) in the disordered state near the ODT (which is expected to have the structure similar to the D_F structure although the real-space analysis was not reported) and for the light scattering profile obtained from the PEP/PEE mixture in the late stage of the SD (Figure 8a) (which is expected to have the sponge-like structure). They found that the scaled profiles, $I(x)/I_m$, plotted as a function of $x \equiv q/q_m$ for the two systems agree quite well with each other in the region of $x < 3$. Thus they concluded that the dynamical structure formed by the concentration fluctuations in the disordered state close to the ODT is essentially same as that in the late stage SD in the homopolymer blend (i.e., the bicontinuous structure composed of PEP-rich and PEE-rich domains with a well-defined interface), though the length scales of these two structures are obviously quite different. This conclusion is qualitatively consistent with our results obtained in Figure 3a. However the plots of the scaled profiles for OSI-3 at 100.1 °C and the PI/polybutadiene (PB) 50/50 (wt/wt) blend in the late stage SD[26,27] (Figure 8b) show the different features from that found by Bates et al., although the scaled profile for the PI/PB blend is almost identical to that for the PEP/PEE blend.

In Figure 8b the scaled profile for OSI-3 in the ordered state obtained at 7285 s after quenching to 97.0 °C is also presented as a reference. Note that the scaled profile of OSI-3 at 100.2 °C is much broader than that in the ordered state at 97.0 °C, as naturally expected. However it is much sharper than that of the PI/PB

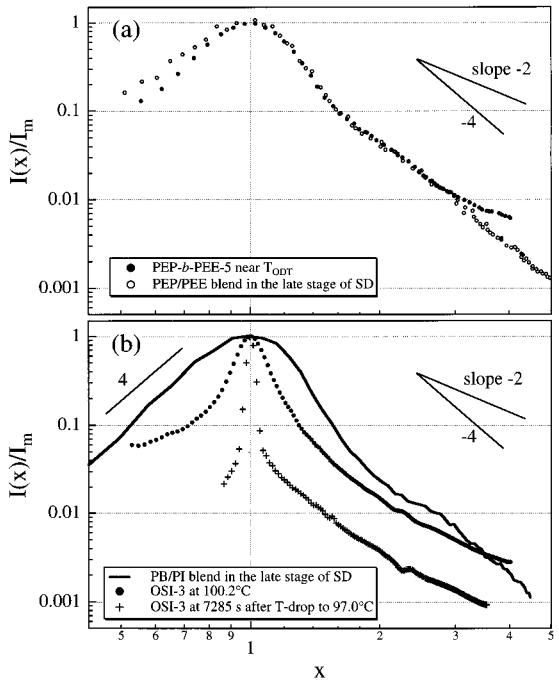

Figure 8. (a) Scaled profiles, $I(x)/I_m$ plotted as a function of $x \equiv q/q_m$ for the PEP-*block*-PEE diblock copolymer, PEP-PEE-5 (●), at a temperature close to the T_{ODT} in the disordered state and the PEP/PEE blend (○) in the late stage of the SD presented in ref 10, and (b) those for the PS-*block*-PI diblock copolymer, OSI-3, at 100.1 °C (●) very close to the T_{ODT} in the disordered state and at 7285 s (+) after quenching to 97.0 °C, and the PB/PI blend (solid line) in the later stage of the SD in ref 27.

blends. The peak width of the scaled profile σ_x is given by $\sigma_x \equiv \sigma_q/q_m$ where σ_q is the peak width of the scattering profile $I(q)$. Now the thermal correlation length of the concentration fluctuations ξ is related to σ_q by $\xi \sim \sigma_q^{-1}$. Hence the scaled correlation length ξ_r defined by $\xi_r = \xi q_m$ is related to σ_x; $\xi_r \sim q_m/\sigma_q = \sigma_x^{-1}$. Thus the sharp peak width in the scaled profile for the OSI-3 at 100.1 °C (i.e., the small σ_x) indicates that the D_F structure has the scaled correlation length ξ_r longer than that of the bicontinuous structures obtained in the late stage SD in the PB/PI and the PEP/PEE blend systems, despite of the fact that the D_F structure is only the dynamical one and that the bicontinuous structures in the polymer blends are static phase-separated structures. This disparity between the scaled structure factor of the polymer blend (PB/PI or PEP/PEE blend) and that of the OSI-3 at 100.1 °C is inconsistent with the observation by Bates et al. Furthermore the peak of PEP-PEE-5 is much broader than that of OSI-3 at 100.1 °C, though both profiles were obtained from the symmetric diblock copolymers in nearly the same conditions, that is, at temperatures very close to T_{ODT} in the disordered state. These disparities may be a surprise and puzzle at first glance. However we may offer our interpretation in the following paragraph.

According to FRH theory,[4] the peak scattered intensity, I_m, at $T_{ODT,H}$ in the disordered state is proportional to $N^{1/3}$ in the context of the Hartree approximation where N is the total degree of the polymerization; hence σ_q is proportional to $N^{-1/6}$ (because $I_m^{-1} \sim \sigma_q^2$). Because $q_m \sim N^{-1/2}$, σ_x is thus proportional to $N^{1/3}$. Here it should be noted that the relationship of $\sigma_x \sim N^{1/3}$ is obtained by assuming that (i) the statistical segment length and the segment volume are identical for each

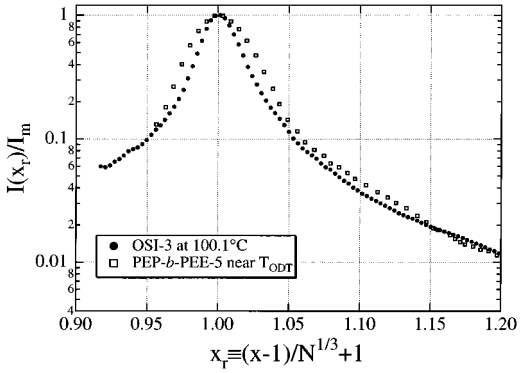

Figure 9. $I(x_r)/I_m$, plotted as a function of $x_r \equiv (q/q_m - 1)/N^{1/3} + 1$ for OSI-3 (●) at 100.1 °C and PEP-PEE-5 (□), both at the temperature close to the T_{ODT} in the disordered state.

block copolymer employed and (ii) the q_m is proportional to $N^{-1/2}$ in addition to the Hartree approximation on the fluctuation effect. Thus we expect that the peak width of the scaled profile for a block copolymer decreases with decreasing N. The width σ_x is sensitive to N when N is small but becomes less sensitive to N at a large limit of N, which may provide a main reason for the disparities as described above.

Figure 9 gives the $I(x_r)/I_m$ plotted as a function of $x_r \equiv (x - 1)/N^{1/3} + 1$ for OSI-3 and PEP-PEE-5 at temperatures very close to T_{ODT} in the disordered state. If σ_x is proportional to $N^{1/3}$, the plots of $I(x_r)/I_m$ versus x_r for block copolymers with various N should fall onto the master profile near the first-order peak. Note in Figure 9 that the peak widths of the two profiles are approximately equal, indicating that the relationship of $\sigma_x \sim N^{1/3}$ is roughly applicable to OSI-3 and PEP-PEE-5 despite the fact that the Hartree approximation is poor for OSI-3 with a small value of N. Thus the difference of the scaled peak width, that is, the difference of the scaled correlation length in OSI-3 and PEP-PEE-5, results from the fact that the N value of OSI-3 ($N = 180$) is much smaller than that of PEP-PEE-5 ($N = 1026$). Another important difference is seen in the second order shoulder, the existance of which indicates an interface in the concentration fluctuations: it exists for PEP-PEE-5 (Figure 8a at $x \cong 2$) but does not exist for OSI-3 (Figure 8b). Thus we can conclude that the D_F structure is close to the spongelike structure, if the N dependence of the scaled peak width is properly taken into account for the D_F structure and if the difference in the reduced interface thickness $\tilde{t}_I \equiv t_I/(2\pi/q_m)$ could be disregarded, where t_I is the interface thickness.

IV-2. Formation of Lamellar Grain. The structure at 330 s after T-drop to 97.0 °C (Figure 3b) is very similar to the D_F structure at 100.1 °C, which is equal to $T_{ODT,H}$ (Figure 3a). Note that the time of 330 s belongs to stage II, that is, the incubation period (see Figure 1). To compare these two structures in reciprocal space, the profiles at 330 s after T-drop to 97.0 and at 100.1 °C are given in Figure 10 over a sufficiently wide q-range. The profiles at 330 s (open circles) at 100.1 °C (crosses) are completely identical except for a difference in the statistical accuracy of data points for the two cases: the system at 100.1 °C is in an equilibrium state so that one can measure the profile over a long exposure time and hence with a high statistical accuracy, while the system at 330 s after T-drop to 97.0 °C is in a nonequilibrium state so that one cannot measure it with the prolonged exposure time; the

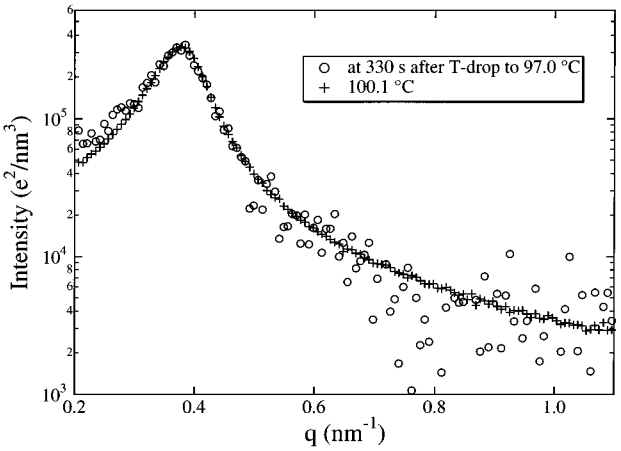

Figure 10. SAXS profiles at 330 s after T-drop to 97.0 °C (○) and at 100.1 °C (+).

exposure time was relatively short (60 s), and hence the statistical accuracy was poor. These features suggest that the system in the incubation period stays in the state close to the equilibrium disordered state at the temperature very close to the T_{ODT} and hence has the D_F structure.

In stage III in which the I_m is increasing (Figure 1), the isolated grains in the matrix of the disordered phase are observed for cases of quenching between 97.0 and 92.5 °C (as shown in Figures 5 and 7 for example). The lamellar grains in Figure 7 are much smaller than those in Figure 5, because the quench depth, ΔT, in the case of 92.5 °C is larger than that of 97.0 °C, making the size of the critical nuclei smaller. The coexistence of the ordered and disorered phases indicates that the ordering proceeded by the nucleation and growth process at all the temperatures covered in this experiment. The ordered grains grow at the expense of the disordered phase.

Furthermore the shapes of the ordered grains developed in the disordered matrix are highly anisotropic as shown in Figures 5 and 7, again at all temperatures covered in this experiment. Recently the shape of the lamellar grains was analyzed theoretically by HS.[22] They estimated the anisotropic interfacial free energy, $\sigma_\perp$ and $\sigma_\parallel$, on the interface between the ordered grain and the matrix of the disordered phase (referred to as OD interface hereafter); that is, they estimated the $\sigma_\perp$ on the transverse interface where the OD interface is perpendicular to the lamellar interfaces and the $\sigma_\parallel$ on the longitudinal interface where the OD interface is parallel to the lamellar interface. They concluded that $\sigma_\perp < \sigma_\parallel$ near the ODT. In this case, the shape of the nucleated lamellar grains is predicted to be anisotropic: the grains are elongated parallel to the lamellar normal. Thus the anisotropic shape of the lamellar grains observed at various T_f values as typically shown in Figures 5 and 7 is consistent with the prediction by HS. This feature in the shape of the lamellar grains was also demonstrated in the computer simulation based on the HS theory.[16] Here it should be mentioned that the shape of the ordered grains highly depends on the type of the microdomain structures, such as a lamella, cylinder, and sphere, because the anisotropy of the interfacial free energy of the OD interface depends on the symmetry of the microdomain structures.[28]

It is worth noting in Figures 5 and 7 that the lamellar structure in the grains has remarkable distortions: the lamellar layers are not solid, showing undulation, bending, and perforation. In the right panel of Figure 7b, the lamellae appear to be composed of the "spots" as illustrated in Figure 11b. These features indicate that the lamellae at the early stage of the ordering process are perforated. Here it should be mentioned that the both lamellae colored by red and violet are perforated in Figure 7b.

On the other hand, at 7285 s after T-drop to 97.0 °C the lamellar grains fill almost all the space as shown in Figure 6. Furthermore most of lamellae are solid and stacked parallel to each other: the distortions as seen in the lamellae in Figure 5 and 7 become minor. The perforated lamellae are transformed into the solid lamellae with time, and the lamellae in the equilibrium state at $97.0 < T < 92.5$ °C are solid and stacked parallel to each other.

Thus we can visualize the ordering process of the lamellar structure induced by T-drop as illustrated in Figure 11. (1) After T-drop, the system stays in the disordered state and has the D_F structure for a certain incubation period (part a). (2) After the incubation period, the lamellar grains develop in the matrix of the disordered phase. The shape of the grains developed in the matrix are elongated parallel to the lamellar normal. Furthermore the lamellae are not solid but perforated in the early stage of the ordering (part b). (3) The perforated lamellae become solid with time (part c), and the lamellar grains get larger. (4) Finally the lamellar grains fill the whole space (part d).

V. Concluding Remarks

We studied the ordering process of the nearly symmetric diblock copolymer with the T-drop method as described in the text and by using TEM, together with the complementary SAXS experiments. The morphologies of the system in the disordered state and in the

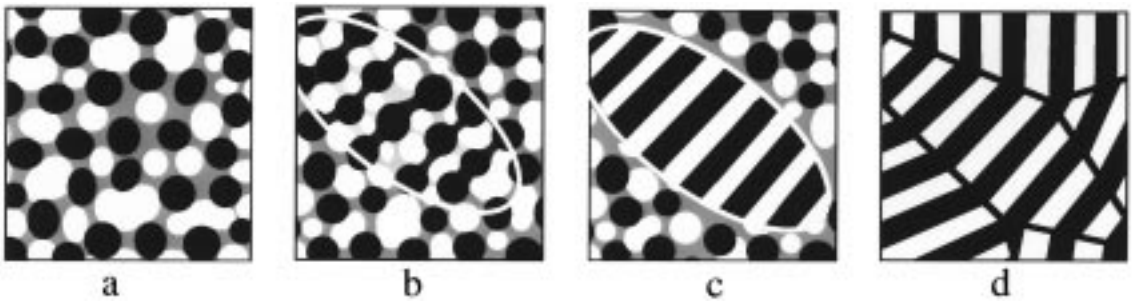

Figure 11. Schematic representation of the formation of the lamellar microdomain after T-drop from the disordered state to the ordered state. In order to highlight the ordered grains composed of the lamellar microdomain, the interface between the ordered grain and the disordered phase in panels b and c and the grain boundaries in the panel d are traced by white and black lines, respectively.

ordering process via nucleation growth were studied by TEM on the specimens frozen at the corresponding state. The complementary SAXS experiments assured that the structures *in situ* before freezing were conserved even after the freezing and staining with O_SO_4 used for the TEM observation. They also helped specify the states where the morphological investigations were performed.

The TEM observation on the specimen frozen from the disordered state very close to the ODT illustrated the fluctuation-induced disordered structure (D_F) as clarified in the text in sections III-1 and IV-1. The TEM observation further revealed that the D_F structure resembles the spongelike 3D-bicontinuous structure developed in the late stage of spinodal decomposition in homopolymer blends. The detailed analysis of the D_F structures with the complementary SAXS investigation, however, indicated that the scaled correlation length of the D_F structure was larger than that of the spongelike structure in the case of the block copolymers with relatively low N. If we properly rescaled the scaled structure factor with this N-dependent scaled correlation length, we found that the rescaled structure factor for the D_F structure is essentially identical to that for the spongelike structure in the polymer blend. Thus the D_F structures turned out to be essentially identical to that for the spongelike structure, except for a difference in sharpness of the interface.

The TEM pictures during the ordering showed that the structure in stage II, that is, the incubation period, is same as that in the D_F structure. In state III where the I_m is increasing in Figure 1, the ordered lamellar grains coexist with the disordered state. The coexistence of the ordered lamellar grains and disordered phase together with the existence of the incubation period observed in the SAXS measurements suggests that the ordering proceeds via nucleation and growth process. Moreover, the shape of the lamellar grains in the matrix of the disordered phase is highly anisotropic: The size along the lamellar normals is much larger than that parallel to the lamellar interfaces. This result is consistent with the prediction by Hohenberg and Swift.[22] The lamellar grains are isolated in the matrix of the disordered phase having the D_F structure and grow at the expense of the disordered phase. The system is eventually volume filled with the ordered grains having anisotropic shape. The lamellae in the ordered grains at the beginning of stage III where the I_m is increasing in Figure 1 has distortion; that is, they are perforated, but they are transformed into the solid lamellae with time.

Acknowledgment. This work was supported in part by Research Fellowships of the Japan Society for the Promotion of Science (JSPS) for Young Scientists (6608) and by a Grant-in-Aid for JSPS fellows (00086608) and Scientific Research on Priority Area, "Cooperative Phenomenon in Complex Liquids" (07236103) from the Ministry of Education, Science, Sports, and Culture, Japan.

References and Notes

(1) See for example a review article: Hashimoto, T. *Thermoplastic Elastomers*; Legge, N. R., Holden, G. R., Schroeder, H. E., Eds.; Hanser: Vienna, 1987; Chapter 12, Sec. 3, 1st ed., and 1996, Chapter 15A, 2nd Ed., and references cited therein.
(2) See for example a review article: Bates, F. S.; Fredrickson, G. H. *Annu. Rev. Phys. Chem.* **1990**, *41*, 525 and references cited therein.
(3) Leibler, L. *Macromolecules* **1980**, *13*, 1602.
(4) Fredrickson, G. H.; Helfand, E. *J. Chem. Phys.* **1987**, *87*, 697.
(5) Brazovskii, A. *Sov. Phys. JETP* **1975**, *41*, 85.
(6) Stühn, B.; Mutter, R.; Albrecht, T. *Europhys. Lett.* **1992**, *18*, 427.
(7) Wolff, T.; Burger, C.; Ruland, W. *Macromolecules* **1993**, *26*, 1707.
(8) Hashimoto, T.; Ogawa, T.; Han, C. D. *J. Phys. Soc. Jpn.* **1994**, *63*, 2206.
(9) Sakamoto, N.; Hashimoto, T. *Macromolecules* **1995**, *28*, 6825.
(10) Bates, F. S.; Rosedale, J. H.; Fredrickson, G. H. *J. Chem. Phys.* **1990**, *92*, 6255.
(11) Rosedale, J. H.; Bates, F. S.; Almdale, K.; Mortensen, K.; Wignall, D. *Macromolecules* **1995**, *28*, 1429.
(12) Fredrickson, G. H.; Binder, K. *J. Chem. Phys.* **1989**, *91*, 7265.
(13) Schuler, M.; Stühn, B. *Macromolecules* **1993**, *26*, 112.
(14) Stühn, B.; Vilesov, A.; Zachmann, H. G. *Macromolecules* **1994**, *27*, 3560.
(15) Hashimoto, T.; Sakamoto, N. *Macromolecules* **1995**, *28*, 4779.
(16) Hashimoto, T.; Sakamoto, N.; Koga, T. *Phys. Rev. E.* **1996**, *54*, 5832.
(17) Sakamoto, N.; Hashimoto, T. *Busseikennkyu* **1996**, *66*, 448.
(18) Rosedale, J. H.; Bates, F. S. *Macromolecules* **1990**, *23*, 2329.
(19) Floudas, G.; Pakula, T.; Fischer, E. W.; Hadiichristidis, N.; Pispas, S. *Acta Polym.* **1994**, *45*, 176.
(20) Floudas, G.; Fytas, G.; Hadichristidis, N.; Pitsikalis, M. *Macromolecules* **1995**, *28*, 2359.
(21) Dai, H. J.; Balsara, B. A.; Garetz, B. A.; Newstein, M. C. *Phys. Rev. Lett.* **1996**, *77*, 3677.
(22) Hohenberg, P. C.; Swift, J. B. *Phys. Rev. E* **1995**, *52*, 1828.
(23) Sakamoto, N.; Hashimoto, T. *Macromolecules*, in press.
(24) Jinnai, H.; Nishikawa, Y.; Koga, T.; Hashimoto, T. *Macromolecules* **1995**, *28*, 4782.
(25) Hashimoto, T.; Jinnai, H.; Nishikawa, Y.; Koga, T.; Takenaka, M. *Progr. Colloid Polym. Sci.* **1997**, *106*, 118.
(26) Takenaka, M.; Hashimoto, T.; Jinnai, H. *J. Appl. Crystallogr.* **1991**, *24*, 457.
(27) Takenaka, M.; Hashimoto, T. *J. Chem. Phys.* **1992**, *96*, 6177.
(28) Sakamoto, N.; Hashimoto, T. Submitted for publication in Macromolecules.

MA980037S